International Journal for Modern Trends in Science and Technology
Volume 10, Issue 05, pages 134-141.
ISSN: 2455-3778 online
Available online at: http://www.ijmtst.com/vol10issue05.html
DOI: https://doi.org/10.46501/IJMTST1005020

A New Multi-Output DC-DC Converter for Electrical Vehicle Application

Thati Venkata M. Lakshmi[1] | Ravi Kumar Guduru[1] | Vallabhaneni Yakshitha[2] | Malladi Sujatha[2] | Boddu Sravani[2] | Kondapalli Avinash[2]

[1]Assistant Professor, Department of Electrical and Electronics Engineering, SRK Institute of Technology-Enikepadu, Vijayawada-521108, Andhra Pradesh, India
[2]Department of Electrical and Electronics Engineering, SRK Institute of Technology-Enikepadu, Vijayawada-521108, Andhra Pradesh, India

To Cite this Article
Thati Venkata M. Lakshmi, Ravi Kumar Guduru, Vallabhaneni Yakshitha, Malladi Sujatha, Boddu Sravani and Kondapalli Avinash2, A New Multi-Output DC-DC Converter for Electrical Vehicle Application, International Journal for Modern Trends in Science and Technology, 2024, 10(05), pages. 134-141. https://doi.org/10.46501/IJMTST1005020

Article Info
Received: 26 April 2024; Accepted: 17 May 2024; Published: 19 May 2024.

ABSTRACT

Multiport converters are essential in portable electronic and electric vehicle (EV) applications. Various single-input multi-output (SIMO) converter configurations have been explored in the literature. Typically, these converters produce outputs under constraints related to duty ratio and inductor charging. However, cross-regulation remains a significant challenge in SIMO converter design. This study proposes a novel SIMO topology to address these limitations. The proposed topology can generate three different output voltages without constraints on the duty cycle and inductor currents (e.g., iL1 > iL2 > iL3 or iL1 < iL2 < iL3). This design eliminates cross-regulation issues, ensuring that the load voltages V01, V02, and V03 are unaffected by variations in the output currents i01, i02, and i03, respectively. The loads are isolated from each other during control. A 200 W prototype circuit was developed and tested in the laboratory, with both simulation and experimental results confirming the effectiveness of the proposed design.

1.INTRODUCTION

Over the past decade, there has been a growing demand for renewable energy sources in electric vehicles (EVs), auxiliary power, and grid-connected applications. Multiport DC-DC converters are crucial in these contexts as they enable hybridizing energy sources, reducing component count, system complexity, and costs compared to using several separate single-input DC-DC converters.

Several multiport converter (MPC) designs have been introduced over the years. For instance, a new single-input multi-output (SIMO) converter structure has been proposed, capable of simultaneously generating boost, buck, and inverted outputs that can be controlled independently. However, generating 'n' voltage levels requires n + 2 switches, increasing the overall size and cost of the converter. Issues with

calculating state-space equations and output voltages for a SIMO converter have been identified and corrected.

A single coupled inductor-based SIMO buck converter has been developed, offering lower output inductor current ripple compared to single inductor SIMO converters. Nayak and Nath have presented a detailed comparison of single-input dual-output (SIDO) converters using coupled and single inductors, highlighting that the coupled inductor SIDO converter performs better in both steady-state and transient conditions. Conversely, in single inductor SIMO configurations, the inductor switching between loads causes high ripples and cross-regulation problems.

Various control strategies have been proposed to address cross-regulation in single inductor-based SIMO converters. For instance, a current predictor controller has been introduced as an alternative to the conventional charge balance approach, though generating duty ratios for active switches remains complex. Similarly, a deadbeat-based control approach, which relies on an output current observer, is sensitive to noise and significant parametric variations. A multivariable digital controller-based SIMO converter has been suggested to minimize voltage ripples and suppress cross-regulation issues, though this approach increases design complexity.

A non-isolated single-switch SIMO converter topology has been proposed, featuring fewer components and lower system costs, although independently regulating the outputs can be challenging. To address these issues, a non-isolated SIMO converter has been developed that independently regulates output voltages without requiring an additional control circuit.

Additionally, a new SIDO converter topology integrating buck and super lift converters has been proposed for generating step-up and step-down output voltages in EV applications, though it imposes duty ratio constraints (D2 < D1), limiting the operational range of D1 by increasing D2. High gain step-up and SEPIC converter-based SIMO designs have been suggested for photovoltaic (PV) applications, which improve output voltage by adding capacitors and diodes but also increase costs and conduction losses.

A new SIDO buck-boost topology has been developed to generate positive and negative outputs. A multi-output converter with a reduced part count has been suggested, though it includes more diodes, increasing conduction losses. A SIMO configuration has been introduced, reducing passive filter size and voltage stress. A high-density multi-output converter has been proposed for portable electronics, based on a front-end switched-capacitor technique that improves power density and reduces switching losses. Modified SEPIC and interleaved high step-up SIMO converters have been introduced, incorporating voltage multipliers, coupled inductors, and switched capacitors to boost output voltage in sustainable energy applications, though they are complex due to the number of components involved.

The SEPIC-Cuk converter-based four-phase interleaved converter has been recommended for SIMO applications, offering low ripple voltage, compact size, and suitability for high power applications with a dynamic response. In conventional EV auxiliary power supply systems, the main drawback is cross-regulation problems, and loads are not isolated from each other during operation. There is also a risk of grounding issues when charging the battery with simultaneously turned-on loads. Additionally, circuit complexity increases when converting one of the negative output voltages into buck-boost operation mode.

The proposed work focuses on an onboard power converter configuration, where the energy stored in the inductor is confined to one output and not shared with other outputs during control, allowing for independent regulation of output voltages with separate duty cycles.

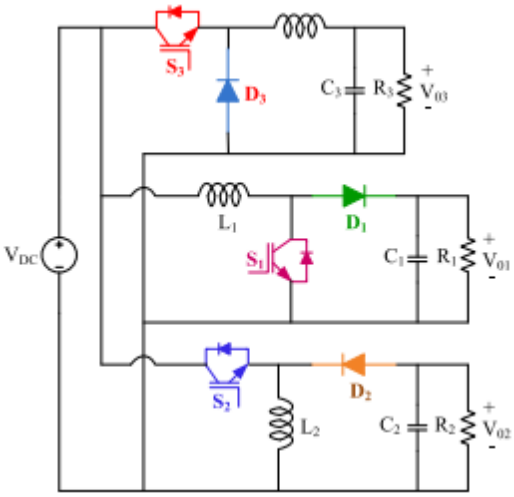

Figure 1: Diagram of Conventional SIMO Converter

2. LITERATURE SURVEY

This article presents a single-inductor multiple-output (SIMO) buck/boost DC-DC converter utilizing average-current control. The proposed design employs a

duty-cycle and control-current predictor to achieve fast and robust reference tracking of inductor current. A modification of the conventional charge-balance method, along with an auto-tuning-divider-based duty generator, mitigates cross-regulation to the last channel. Additionally, an anti-right-half-plane zero method is introduced to suppress cross-regulation during significant load transients in boost mode. The SIMO buck/boost converter features four output channels, adaptable to both boost and buck operations, and is implemented using a standard 0.35-μm CMOS process. Measurement results indicate a peak efficiency exceeding 89% at a total output power of approximately 0.5 W, a load transient response time of less than 40 μs, and cross-regulation within 0.05 V/A during a 300-mA load transient applied to a boost channel.

2.1.1 Super-Lift Luo-Converter (2021)

This paper introduces a DC-DC multi-port converter integrating a super-lift and a buck converter (SLBC). The proposed single-input dual-output (SIDO) converter combines the positive output voltage super-lift advantages with the capability of generating step-up and step-down voltages via the Luo and buck converters, respectively. The SLBC structure maintains low ripple in output voltages without electromagnetic components, and features a simple design and control method, offering a wide range of output voltages. Comparative analysis with similar configurations highlights the advantages of the SLBC, including reduced conduction losses. Simulation and experimental results validate the performance and accuracy of the SLBC, with several tests conducted in PSCAD/EMTDC software and a 150W prototype tested in the laboratory.

2.1.2 Integrated Multiple-Output Synchronous Buck Converter (2017)

This paper proposes a novel integrated synchronous buck converter for EV auxiliary power systems, achieving multiple independently regulated outputs with fewer switching components compared to conventional separate buck converters. A detailed examination of a simplified dual-output buck converter demonstrates the operational principle and performance characteristics, achieving zero-voltage-switching and lower conduction losses. The dynamic behavior is akin to conventional buck converters, simplifying controller design. Experimental results from a prototype circuit, where two inductors are integrated into a single magnetic core, further verify the advantages, including cost reduction.

2.1.3 New Dual Output DC-DC Converter with Enhanced Output Voltage Level (2016)

This paper proposes a new dual-output DC-DC converter derived from a conventional design with minor modifications. Unlike traditional dual-output converters that provide identical voltage levels, this topology offers different voltage levels, with one output voltage significantly increased. The converter employs two switches for power conversion without transformers, serving as an alternative to two single-output power supplies. Detailed steady-state analysis and MATLAB Simulink simulations verify the theoretical analysis.

2.1.4 Novel Single-Input Dual-Output Three-Level DC-DC Converter (2018)

This paper introduces a non-isolated single-input dual-output three-level DC-DC converter (SIDO-TLC) suitable for medium- and high-voltage applications. The SIDO-TLC integrates three-level buck and boost converters, simultaneously regulating output voltages. Benefits include reduced voltage stress on semiconductor devices, improved efficiency, and smaller inductor sizes. The design also minimizes the volume of the step-down filter capacitor, allowing the use of small film capacitors with lower equivalent series resistance and longer lifespans. A closed-loop control system ensures regulated output voltages and capacitor voltage balancing. Theoretical and simulation results are verified with a 300W prototype, demonstrating the advantages and stability of the SIDO-TLC even under simultaneous load and input voltage changes.

2.1.5 Interleaved Single-Input Multiple-Output DC-DC Converter Combination

This paper explores a four-phase interleaved DC-DC converter based on a SEPIC-Cuk combination, designed for SIMO applications. The prototype delivers dual output voltages from a single input DC voltage with a single power switch. Multiphase interleaved converters enhance dynamic response and reduce ripple, distributing losses across multiple components for

improved thermal management and high power handling in compact sizes. Two control strategies—synchronous operation mode (SOM) and interleaved operation mode (IOM)—were applied and tested.

3. PROPOSED SIMO CONVERTER

The proposed single input three-output DC-DC configuration is depicted in Figure 2. In this configuration the components are as follows, input voltage VDC, switches (S1-S3), diodes (D1-D3), and passive elements (L1-C1, L2-C2, and L3-C3). It can generate three different output voltages, i.e., boost (V01), buck-boost (V02) with positive voltage polarity, and buck (V03). The proposed converter is suitable for independently regulating the output voltages by the duty cycles D1, D2, and D3, respectively. The theoretical waveforms of circuit elements are depicted in Figure 2(b). The proposed configuration is different from the conventional parallel combination of buck, boost, and buck-boost configuration. In the proposed circuit configuration, the loads are isolated during the simultaneous control. From the following figures, one may observe that during mode-1operation, load R3 alone through S3 is connected to the input power supply, but the other loads are isolated, as shown in Figure 3(a). Similarly, during mode-2 only load R1 alone through D1 is connected to the input supply, but other loads are isolated, as depicted in Figure 3(b). In the proposed control strategy, all the loads are isolated from each other during their control in any mode of operation. However, this feature is impossible in the conventional parallel combination of buck, boost, and buck-boost converters,

In the conventional approach shown in Figure1, the main drawback is the cross-regulation problem, and the loads are not isolated from each other during their operation. Further, the circuit complexity will increase to convert the negative polarity of output voltages in the buck-boost mode of operation. The proposed structure has the following advantages:

a) It is a simple structure and no assumptions on operating duty ratio (D1 > D2 > D3 or D3 < D2 < D1 or D1 = D2 = D3)

b) It can generate three different output voltages, i.e., boost, buck, buck-boost()

c) No constraints on inductor currents (like iL1 > iL2 > iL3 or iL1 < iL2 < iL3 or iL1 = iL2 = iL3)

d) Loads are isolated from each other during control and the cross-regulation problem is successfully eliminated

e) It gives the positive buck-boost output voltage

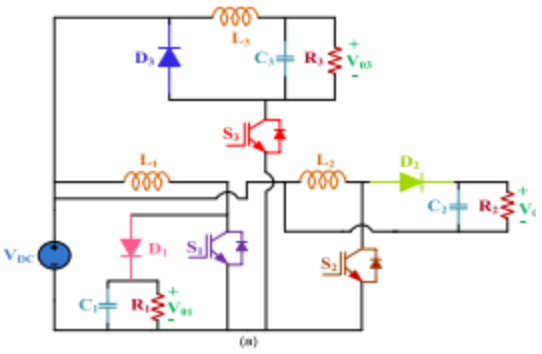

Figure 2 : Proposed SIMO Converter

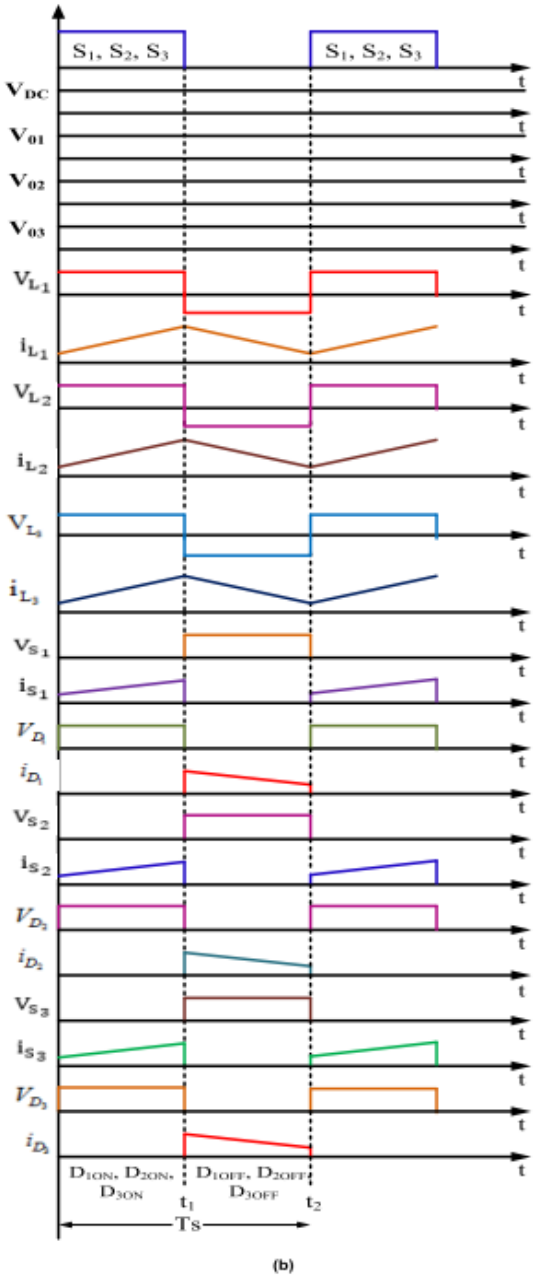

Figure 3: Theoretical Waveforms

3.1 MODES OF OPERATION

3.1.1Switching state 1

Switches S1, S2, and S3 are turned ON. The current flow path is depicted in Figure 3(a), and the energy port VDC magnetizes L1, L2, and L3. Consequently, the C1 and C2 are discharged to the loads (R1) and (R2), respectively, whereas (C3) is charged. The inductor currents and capacitor voltages are represented

$$i_{L_1}(t) = \frac{V_{DC}}{L_1}t + i_{L_1(0)}, \quad v_{C_1}(t) = v_{C_1(0)}e^{\frac{-1}{R_1C_1}t} \tag{1}$$

$$i_{L_2}(t) = \frac{V_{DC}}{L_2}t + i_{L_2(0)}, \quad v_{C_2}(t) = v_{C_2(0)}e^{\frac{-1}{R_2C_2}t} \tag{2}$$

$$i_{L_3}(t) = \frac{V_{DC}}{R_3} + e^{-\alpha t}\left[c_1 \cos \omega_d t + c_2 \sin \omega_d t\right] \tag{3}$$

$$v_{C_3}(t) = V_{DC} - \frac{L_3}{2C_3}e^{-\alpha t}\begin{bmatrix}\cos \omega_d t(\frac{\alpha c_1}{R_3} + \omega_d c_2) \\ + \sin \omega_d t(-\alpha c_2 + \frac{\omega_d c_1}{R_3})\end{bmatrix} \tag{4}$$

3.1.2 Switching state 2

In this state, L1, L2, and L3 are de-magnetized and deliver their energy to the load through D1, D2, and D3, respectively. It is illustrated .The inductor currents and capacitor voltages,

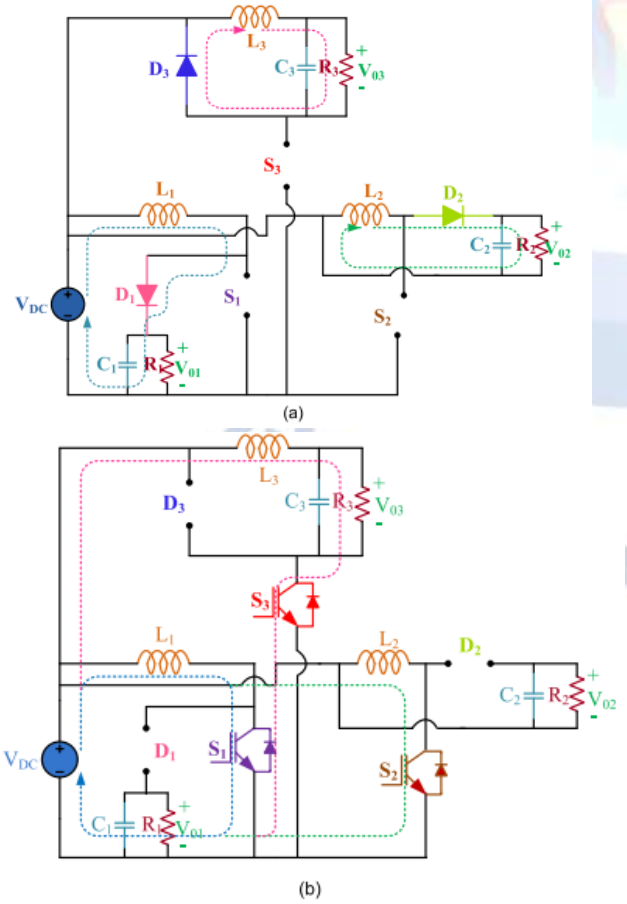

Figure 4: Operating States: (a) Switching State-1 And (b) Switching State-2.

$$i_{L_1}(t) = \frac{V_{DC}}{R_1} + e^{-\alpha_1 t}\left[c_1 \cos \omega_{d1} t + c_2 \sin \omega_{d1} t\right] \tag{5}$$

$$v_{C_1}(t) = V_{DC} - \frac{L_1}{2C_1}e^{-\alpha_1 t}\begin{bmatrix}\cos \omega_{d1} t(\frac{c_1}{R_1} - \omega_{d1} c_2) \\ + \sin \omega_{d1} t(\omega_{d1} c_1 + \frac{c_2}{R_1})\end{bmatrix} \tag{6}$$

$$i_{L_2}(t) = e^{-\alpha_2 t}\left[c_3 \cos \omega_{d2} t + c_4 \sin \omega_{d2} t\right] \tag{7}$$

$$v_{C_2}(t) = -L_2 e^{-\alpha_2 t}\begin{bmatrix}(-\alpha_2 c_3 + \omega_{d2} c_4) \cos \omega_{d2} t \\ + (\omega_{d2} c_3 - \alpha_2 c_4) \sin \omega_{d2} t\end{bmatrix} \tag{8}$$

$$i_{L_3}(t) = e^{-\alpha t}\left[c_5 \cos \omega_d t + c_6 \sin \omega_d t\right] \tag{9}$$

$$v_{C_3}(t) = -L_3 e^{-\alpha t}\begin{bmatrix}(-\alpha c_5 + \omega_d c_6) \cos \omega_d t \\ + (\omega_d c_5 - \alpha c_6) \sin \omega_d t\end{bmatrix} \tag{10}$$

$$\alpha_1 = \frac{1}{2R_1C_1}, \quad \omega_{d1} = \frac{1}{2}\sqrt{\left(\frac{1}{R_1^2C_1^2} - \frac{4}{L_1C_1}\right)},$$

$$\alpha_2 = \frac{1}{2R_2C_2} \quad \text{and } \omega_{d2} = \frac{1}{2}\sqrt{\left(\frac{1}{R_2^2C_2^2} - \frac{4}{L_2C_2}\right)}$$

$$\alpha = \frac{1}{2R_3C_3}, \quad \omega_d = \frac{1}{2}\sqrt{\left(\frac{1}{R_3^2C_3^2} - \frac{4}{L_3C_3}\right)}, \tag{11}$$

where c1, c2, c3, c4, c5, and c6 areinitial values. Output voltages of the proposed configuration are as follows

$$V_{01} = \frac{V_{DC}}{(1 - D_1)}, \quad V_{02} = \frac{V_{DC}D_2}{(1 - D_2)}, \; V_{03} = D_3 V_{DC} \tag{12}$$

D1, D2, and D3 are duty ratios of the S1, S2, and S3 respectively. It is observed that during switching state-1operation, load (R3) alone through S4 is connected to the ground but the other loads are isolated even when the ground is involved during charging the battery, as shown in Figure 3(a). Similarly, during switching state-2 only load (R1) alone through D1 is connected to the ground, but other loads are isolated from the ground and the load (R1) as well as depicted in Figure 3(b). In the proposed control strategy, all the loads are isolated from each other during their control during any mode of operation. Moreover, the configuration of the circuit is such that energy stored in the inductor is confined to one output only and is not shared with the other outputs during the control and also, which allows controlling the output voltages with independent duty-cycles. As a result, the load voltage V01 (V02) (V03) is not influenced by the variation of load current i03 (i02) (i01). Hence the proposed configuration with this control approach

avoids all the issues about crossregulation problems even when the ground is involved during battery charging. More importantly, the configuration is simple and it can generate three independent outputs without any assumptions on inductor currents (iL1 > iL2 > iL3 or iL1 < Il

4. SIMULATION RESULTS

The model has been built in MATLAB environment to verify the proposed system with VDC = 50 V, frequency is 50 kHz, and the duty ratio is 50%. The parameter details are specified in Table. 2. The corresponding output voltages (V01, V02, and V03) and inductor currents (iL1, iL2, and iL3) are illustrated in Figure 6(a-f), respectively. The output voltages in Figures 5(a), 5(c) 5(e) are close to the theoretical results. The closed-loop control is implemented for the proposed configuration, and the dynamic performance of the overall system is validated for a sudden change in the input voltage. Figure 6. shows the simulation result of closed-loop control for a sudden change in the input voltage (VDC) from 50V to 70 V at 0.5 sec. The PI control gains are chosen as Kp = 0.1 and Ki = 15 for Buck output, similarly Kp = 0.005 and Ki = 0.5 for Boost and Buck-Boost voltages. The results show that the proposed configuration generates stiff independent output voltages and is not affected by the sudden change in supply. The efficiency of the proposed converter at different duty ratios and various power ratings is depicted in Figure 7.

Proposed converter connected to EV

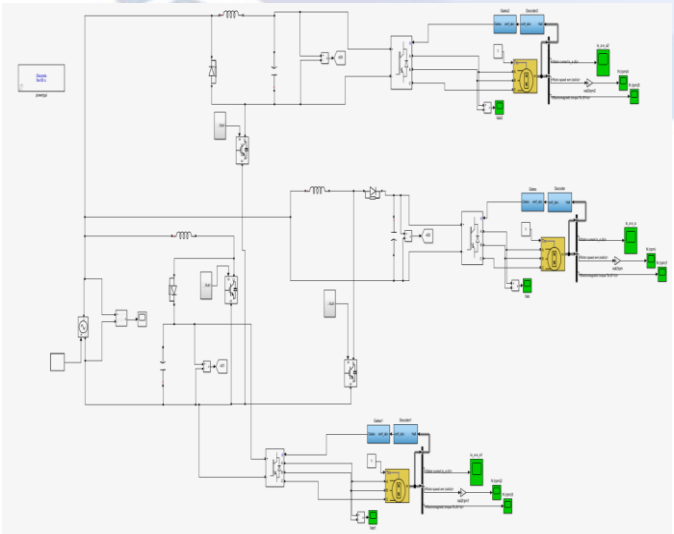

FIGURE 5: SIMULATION OF PROPOSED CONVERTER CONNECTED TO EV

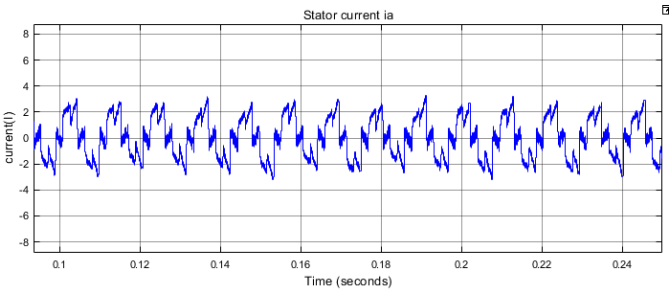

FIGURE 6: STATOR CURRENT OF PHASE 1

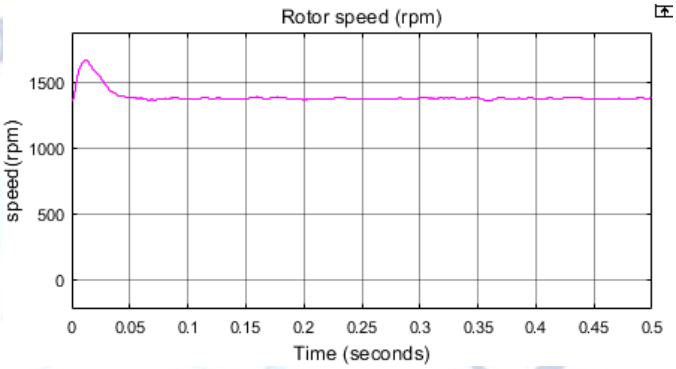

FIGURE 7: ROTOR SPEED PHASE 1

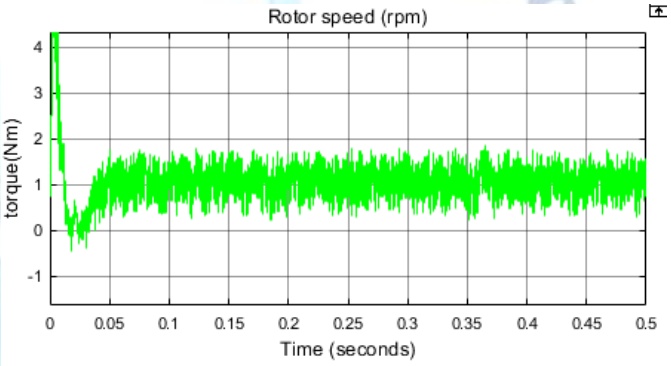

FIGURE 8 : TORQUE OF PHASE 1

Battery discharging in EV

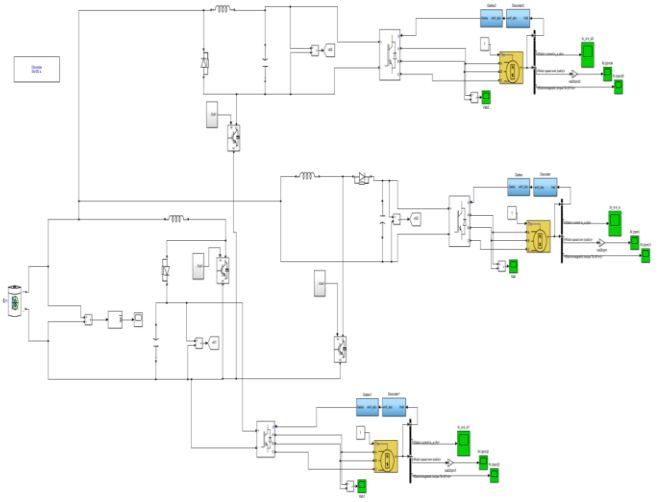

FIGURE 9: SIMULATION OF BATTERY DISCHARGING IN EV

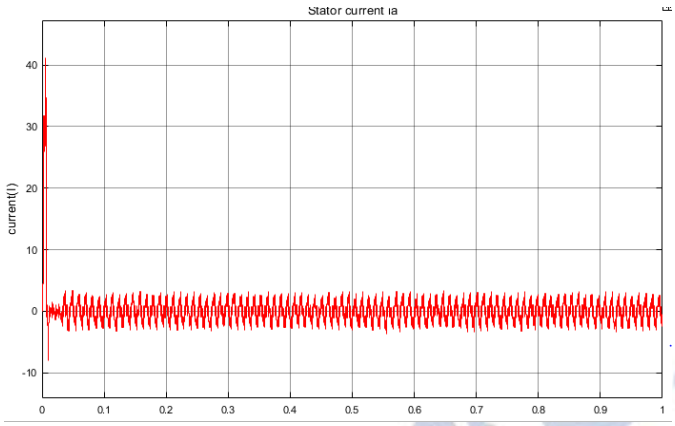

FIGURE 10: STATOR CURRENT IN PHASE 1

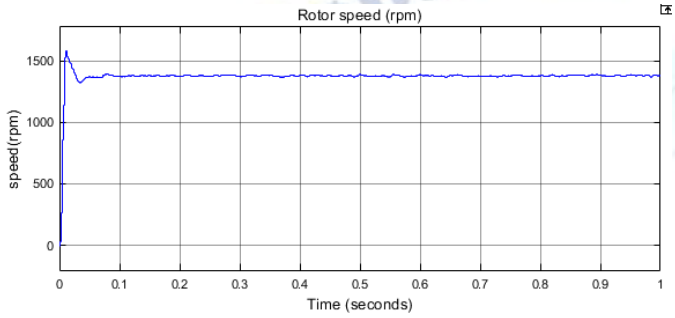

FIGURE 11: ROTOR SPEED IN PHASE 1

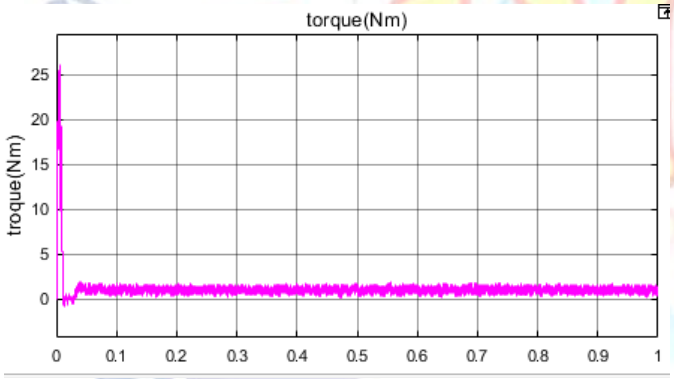

FIGURE 12: ELECTROMAGNETIC TORQUE IN PHASE 1

5. CONCLUSION

In this paper, we propose a novel structure for a single-inductor multiple-output (SIMO) converter. We provide a comprehensive explanation of its operating principle and the various modes of operation. The proposed SIMO converter configuration is straightforward, free from assumptions regarding inductor charging and operating duty cycles. It is designed to generate buck, boost, and buck-boost output voltages with independently regulated voltages for each output.

One of the key advantages of this proposed topology is the elimination of cross-regulation problems. In traditional SIMO converters, sudden changes in inductor and load currents can adversely affect the output voltages, leading to instability and inefficiency. However, the design of our proposed converter ensures that these sudden changes do not impact the output voltages, maintaining consistent and reliable performance.

To validate the effectiveness of the proposed SIMO converter, we conducted extensive simulations and experimental tests. The results from these simulations and experiments confirm that the converter operates as intended, providing robust and stable output voltages across various conditions. The successful validation of the proposed converter highlights its potential for practical applications in systems requiring multiple regulated voltages from a single inductor, such as portable electronics and electric vehicles.

Overall, this paper presents a detailed and thorough investigation into the proposed SIMO converter, demonstrating its advantages in terms of simplicity, independent voltage regulation, and resilience to cross-regulation issues. The experimental and simulation results further reinforce the practicality and effectiveness of the proposed design.

Conflict of interest statement

Authors declare that they do not have any conflict of interest.

REFERENCES

[1] P. C. Heris, Z. Saadatizadeh, and E. Babaei, ''A new two input-single output high voltage gain converter with ripple-free input currents and reduced voltage on semiconductors,'' IEEE Trans. Power Electron., vol. 34, no. 8, pp. 7693–7702, Aug. 2019, doi: 10.1109/TPEL.2018.2880493.

[2] A. Farakhor, M. Abapour, and M. Sabahi, ''Design, analysis, and implementation of a multiport DC–DC converter for renewable energy applications,'' IET Power Electron., vol. 12, no. 3, pp. 465–475, Mar. 2019.

[3] S. K. Mishra, K. K. Nayak, M. S. Rana, and V. Dharmarajan, ''Switchedboost action based multiport converter,'' IEEE Trans. Ind. Appl., vol. 55, no. 1, pp. 964–975, Jan./Feb. 2019.

[4] X. Lu, K. L. V. Iyer, C. Lai, K. Mukherjee, and N. C. Kar, ''Design and testing of a multi-port sustainable DC fast-charging system for electric vehicles,'' Electr. Power Compon. Syst., vol. 44, no. 14, pp. 1576–1587, Aug. 2016.

[5] E. Babaei and O. Abbasi, ''A new topology for bidirectional multi-input multi-output buck direct current–direct current converter,'' Int. Trans. Electr. Energ. Syst., vol. 27, no. 2, pp. 1–15, Feb. 2017.

[6] Z. Rehman, I. Al-Bahadly, and S. Mukhopadhyay, ''Multiinput DC–DC converters in renewable energy applications—An

overview,'' Renew. Sustain. Energy Rev., vol. 41, pp. 521–539, Jan. 2015.

[7] G. Chen, Y. Liu, X. Qing, and F. Wang, ''Synthesis of integrated multi-port DC–DC converters with reduced switches,'' IEEE Trans. Ind. Electron., vol. 67, no. 6, pp. 4536–4546, Jun. 2019.

[8] P. Patra, A. Patra, and N. Misra, ''A single-inductor multiple-output switcher with simultaneous buck, boost, and inverted outputs,'' IEEE Trans. Power Electron., vol. 27, no. 4, pp. 1936–1951, Apr. 2012.

[9] M. Abbasi, A. Afifi, and M. R. A. Pahlavani, ''Comments on 'a singleinductor multiple-output switcher with simultaneous buck, boost, and inverted outputs,''' IEEE Trans. Power Electron., vol. 34, no. 2, pp. 1980–1984, Feb. 2019.

[10] Y.-C. Hsu, J.-Y. Lin, C.-H. Wang, and S.-W. Chou, ''An SIMO stepdown converter with coupled inductor,'' in Proc. Int. Symp. VLSI Design, Autom. Test (VLSI-DAT), Hsinchu, Taiwan, Aug. 2020, pp. 1–4, doi: 10.1109/VLSI-DAT49148.2020.9196435.

[11] G. Nayak and S. Nath, ''Comparing performances of SIDO buck converters,'' in Proc. IEEE Int. Conf. Power Electron., Drives Energy Syst. (PEDES), Chennai, India, Dec. 2018, pp. 1–6.

[12] Y. Zheng, J. Guo, and K. N. Leung, ''A single-inductor multiple-output buck/boost DC–DC converter with duty-cycle and control-current predictor,'' IEEE Trans. Power Electron., vol. 35, no. 11, pp. 12022–12039, Nov. 2020.

[13] X. Zhang, B. Wang, X. Tan, H. B. Gooi, H. H.-C. Iu, and T. Fernando, ''Deadbeat control for single-inductor multiple-output DC–DC converter with effectively reduced cross regulation,'' IEEE J. Emerg. Sel. Topics Power Electron., vol. 8, no. 4, pp. 3372–3381, Dec. 2020.

[14] J. D. Dasika, B. Bahrani, M. Saeedifard, A. Karimi, and A. Rufer, ''Multivariable control of single-inductor dual-output buck converters,'' IEEE Trans. Power Electron., vol. 29, no. 4, pp. 2061–2070, Apr. 2014.

[15] E. Durán, S. P. Litrán, and M. B. Ferrera, ''Configurations of DC–DC converters of one input and multiple outputs without transformer,'' IET Power Electron., vol. 13, no. 12, pp. 2658–2670, Sep. 2020.

[16] B. Faridpak, M. Farrokhifar, M. Nasiri, A. Alahyari, and N. Sadoogi, ''Developing a super-lift Luo-converter with integration of buck converters for electric vehicle applications,'' CSEE J. Power Energy Syst., vol. 7, no. 4, pp. 811–820, Jul. 2021, doi: 10.17775/CSEEJPES.2020.01880.

[17] O. Ray, A. Josyula, S. Mishra, and A. Joshi, ''Integrated dual-output converter,'' IEEE Trans. Ind. Electron., vol. 62, no. 1, pp. 371–382, Jan. 2015.

[18] G. Chen, Y. Deng, J. Dong, Y. Hu, L. Jiang, and X. He, ''Integrated multiple-output synchronous buck converter for electric vehicle power supply,'' IEEE Trans. Veh. Technol., vol. 66, no. 7, pp. 5752–5761, Jul. 2017.